

NANOGrav and PPTA Tension: Gravity Waves, Cosmic Strings, and Inflation

George Lazarides,¹ Rinku Maji,² Qaisar Shafi³

¹ *School of Electrical and Computer Engineering, Faculty of Engineering, Aristotle University of Thessaloniki, Thessaloniki 54124, Greece*

² *Indian Institute of Technology Kanpur, Kanpur - 208016, India*

³ *Bartol Research Institute, Department of Physics and Astronomy, University of Delaware, Newark, DE 19716, USA*

Abstract

The NANOGrav collaboration has recently presented its pulsar timing array data which seem compatible with the presence of a stochastic gravity wave background emitted by cosmic strings with a dimensionless string tension $G\mu \simeq 2 \times 10^{-11} - 3 \times 10^{-10}$ at 95% confidence level (G is Newton's constant and μ denotes the string tension). However, there is some tension between these results and the previous pulsar timing array bound $G\mu \lesssim 4 \times 10^{-11}$ from the PPTA experiment. We propose a relaxation of this tension by invoking primordial inflation which partially inflates the string network. The latter re-enters the horizon at later times after the end of inflation, and thus the short string loops are not produced. This leads to a reduction of the gravity wave spectrum which is more pronounced at higher frequencies. The reconciliation of the NANOGrav results with the PPTA bound is possible provided that the strings re-enter the horizon at adequately late times. We consider an example of a realistic $SO(10)$ model incorporating successful inflation driven by a gauge singlet real scalar field with a Coleman-Weinberg potential. This model leads to the production of intermediate scale topologically stable cosmic strings that survive inflation. We show regions of the parameter space where the tension between NANOGrav and PPTA is alleviated. Finally, we present an example in which both monopoles and strings survive inflation with the above tension resolved.

1 Introduction

The existence of topologically stable cosmic strings in grand unified theory (GUT) models such as $SO(10)$ (more precisely $Spin(10)$) has been known for quite some time [1], and their role in cosmology has attracted a fair amount of interest in recent years – see e.g. Refs. [2–7]. The string tension μ , i.e. the energy per unit length of the string, depends on the symmetry breaking pattern of the GUT symmetry and is related to an appropriate intermediate scale M_{str} determined by various phenomenological considerations including gauge coupling unification. The primordial string loops decay by emitting stochastic gravitational radiation [8], and an important constraint on M_{str} arises from the pulsar timing array experiments – see Ref. [9] and references therein. The recently published 12.5 yr pulsar timing array data from the NANOGrav collaboration [10] provides some provisional evidence for the existence of a gravity wave signal at frequencies $f \sim 1 \text{ yr}^{-1}$. It has been recognized by several authors [5, 7, 10] that these data appear compatible with an interpretation in terms of a stochastic gravity wave background emitted by cosmic strings. However, there is some tension between the NANOGrav results and the previous pulsar timing array measurements in this frequency range, especially the ones from the PPTA collaboration [11]. Indeed, the latter measurements require that the dimensionless string tension $G\mu \lesssim 4 \times 10^{-11}$ at 95% confidence level (c.l.) [5, 9], while fits to the recent NANOGrav data estimate that the $G\mu$ value is in the range $(2 - 30) \times 10^{-11}$ with 95% c.l. (G is Newton’s constant).

In this paper we present one way to alleviate the tension between NANOGrav and PPTA. The idea is that the strings are generated in a phase transition during primordial inflation. They are then partially inflated and at some point after the end of inflation, they re-enter the post-inflationary horizon. Their subsequent self interactions produce string loops which emit gravity waves and eventually decay. Under these circumstances, the short loops are absent and, consequently, the gravity wave spectrum at high frequencies is altered. Indeed, as the re-entrance time of the strings approaches the equidensity time, the spectrum of gravity waves at frequencies corresponding to its overall peak or higher is gradually reduced [6]. This is expected to help fulfill the PPTA bound for appropriate $G\mu$ values that also satisfy the NANOGrav limits.

It is interesting to note that $G\mu$ values of order 10^{-11} or so, which are of interest here, require intermediate scales $M_{\text{str}} \sim 10^{14}$ GeV which coincide, more or less, with the values of the Hubble parameter during primordial inflation driven by a gauge singlet real scalar field with a Coleman-Weinberg potential [12, 13]. This fact has been exploited in the past to show how intermediate scale primordial monopoles may survive inflation and appear in the present universe at an observable rate [6, 13, 14]. By the same token, intermediate scale cosmic strings can also survive an inflationary epoch and contribute to the present spectrum of stochastic gravity wave. Therefore, it is instructive to use this particular inflationary model for alleviating the tension between PPTA and NANOGrav. We consider examples of realistic $SO(10)$ and E_6 symmetry breaking patterns that yield topologically stable cosmic strings with $G\mu$ values in the required range. These strings are not inflated away, as we briefly show following our

earlier work [6]. Indeed, the strings re-enter the horizon after inflation and subsequently generate gravity waves. We discuss how inflation could help realize values for $G\mu \gtrsim 1.1 \times 10^{-10}$ compatible with NANOGrav, without running into conflict with the somewhat more stringent bounds on $G\mu$ from the earlier pulsar timing array experiments. In one example, a possibly measurable monopole flux is also predicted.

The paper is organized as follows. In Sec. 2, following closely the discussion in Ref. [6], we summarize the salient features of the inflationary model with a Coleman-Weinberg potential and sketch briefly the intermediate scale phase transition leading to string formation. In Sec. 3 we outline the evolution of the string network and the calculation of the gravity wave spectrum that is generated. In Sec. 4 we fit the power-law approximation of the gravity wave spectrum for various $G\mu$ values both with and without inflation. In the case of inflation, we find the maximum (minimum) horizon re-entrance time of the strings which is compatible with the NANOGrav (PPTA) constraints. Sec. 5 is devoted to the resolution of the tension between NANOGrav and PPTA in realistic non-supersymmetric $SO(10)$ and E_6 models which incorporate inflation with a Coleman-Weinberg potential. A brief discussion of how an observable monopole flux can be compatible with these considerations is presented. Our results are summarized in Sec. 6.

2 Inflation and Phase Transition

We employ an inflationary scenario where the inflaton is a gauge singlet real scalar field ϕ with a Coleman-Weinberg potential [12, 13]

$$V(\phi) = A\phi^4 \left[\log \left(\frac{\phi}{M} \right) - \frac{1}{4} \right] + V_0. \quad (1)$$

Here $V_0 = AM^4/4$, M is the vacuum expectation value (VEV) of ϕ , and $A = \beta^4 D / (16\pi^2)$ [3], where D is the dimensionality of the representation to which the GUT gauge symmetry breaking real scalar field χ belongs, and β determines the coupling $-\beta^2 \phi^2 \chi^2 / 2$ between ϕ and χ . For definiteness, we adopt the particular parameter set $V_0^{1/4} = 1.66 \times 10^{16}$ GeV, $M = 23.81 m_{\text{Pl}}$, and $A = 2.5 \times 10^{-14}$ from Table 6 of Ref. [6] corresponding to a viable inflationary scenario ($m_{\text{Pl}} = 2.4 \times 10^{18}$ GeV is the reduced Planck mass). The inflaton value at the pivot scale $k_* = 0.05 \text{ Mpc}^{-1}$ and at the end of inflation is $\phi_* = 12.17 m_{\text{Pl}}$ and $\phi_e = 22.47 m_{\text{Pl}}$ respectively. The termination of inflation is determined by the condition $\max(\epsilon, |\eta|) = 1$, where ϵ and η are the usual slow-roll parameters (for a review see Ref. [15]).

We assume that the cosmic strings are generated during a phase transition associated with an intermediate step of gauge symmetry breaking by the VEV of the real scalar field χ_{str} . The χ_{str} -dependent part of the potential is

$$V(\phi, \chi_{\text{str}}) = -\frac{1}{2} \beta_{\text{str}}^2 \phi^2 \chi_{\text{str}}^2 + \frac{\alpha_{\text{str}}}{4} \chi_{\text{str}}^4, \quad (2)$$

implying that the VEV of χ_{str} after the end of inflation is given by

$$\langle \chi_{\text{str}} \rangle \equiv M_{\text{str}} = \frac{\beta_{\text{str}}}{\sqrt{\alpha_{\text{str}}}} M. \quad (3)$$

During inflation, the finite temperature corrections to the potential in Eq. (2) contribute an additional term $(1/2)\sigma_{\chi_{\text{str}}}T_H^2\chi_{\text{str}}^2$, where $\sigma_{\chi_{\text{str}}}$ is of order unity and $T_H = H/2\pi$ is the Hawking temperature, with H being the Hubble parameter. Two symmetric minima of the potential appear at

$$\chi_{\text{str}} = \pm\sqrt{(\beta_{\text{str}}^2\phi^2 - \sigma_{\chi_{\text{str}}}T_H^2)/\alpha_{\text{str}}} \quad (4)$$

as ϕ grows sufficiently large. The effective mass m_{eff} of χ_{str} at these minima is given by

$$m_{\text{eff}}^2 = 2(\beta_{\text{str}}^2\phi^2 - \sigma_{\chi_{\text{str}}}T_H^2). \quad (5)$$

The phase transition during which the intermediate gauge symmetry breaking is completed and the strings are formed occurs when the Ginzburg criterion [16]

$$\frac{4\pi}{3}\xi^3\Delta V = T_H \quad (6)$$

is satisfied (for details see Ref. [6]). Here

$$\Delta V = \frac{1}{4\alpha_{\text{str}}}(\beta_{\text{str}}^2\phi^2 - \sigma_{\chi_{\text{str}}}T_H^2)^2 = \frac{m_{\text{eff}}^4}{16\alpha_{\text{str}}} \quad (7)$$

is the potential energy difference between the minima in Eq. (4) and the local maximum at $\chi_{\text{str}} = 0$, and

$$\xi = \min(H^{-1}, m_{\text{eff}}^{-1}) \quad (8)$$

is the correlation length. Using Eqs. (6), (7), and (8), one can show that $m_{\text{eff}}^{-1} \leq H^{-1}$ implies that $\alpha_{\text{str}} \geq \pi^2/6$ and $m_{\text{eff}}^{-1} \geq H^{-1}$ implies that $\alpha_{\text{str}} \leq \pi^2/6$. In the former case, $\xi = m_{\text{eff}}^{-1}$ and the Ginzburg criterion in Eq. (6) takes the form

$$\beta_{\text{str}}^2\phi^2 = \left(\frac{72\alpha_{\text{str}}^2}{\pi^2} + \sigma_{\chi_{\text{str}}}\right)T_H^2. \quad (9)$$

The intermediate symmetry breaking scale can then be expressed as

$$M_{\text{str}} = \sqrt{\left(\frac{72\alpha_{\text{str}}^2}{\pi^2} + \sigma_{\chi_{\text{str}}}\right)}\frac{H_{\text{str}}}{2\pi\phi_{\text{str}}}\frac{M}{\sqrt{\alpha_{\text{str}}}}, \quad (10)$$

where ϕ_{str} is the inflaton field value at the phase transition, $H_{\text{str}} = \sqrt{V(\phi_{\text{str}})/3m_{\text{Pl}}^2}$ is the corresponding value of the Hubble parameter, and we set $\sigma_{\chi_{\text{str}}} = 1$. On the other hand, for $\alpha_{\text{str}} \leq \pi^2/6$, Eq. (6) gives

$$M_{\text{str}} = \sqrt{\left(2\sqrt{6}\pi\alpha_{\text{str}}^{\frac{1}{2}} + \sigma_{\chi_{\text{str}}}\right)}\frac{H_{\text{str}}}{2\pi\phi_{\text{str}}}\frac{M}{\sqrt{\alpha_{\text{str}}}}. \quad (11)$$

3 Cosmic Strings and Gravity Waves

The dimensionless tension of the cosmic strings formed during the symmetry breaking at the intermediate scale M_{str} is [17]

$$G\mu \simeq \frac{1}{8}B\left(\frac{\alpha_{\text{str}}}{g^2}\right)\left(\frac{M_{\text{str}}}{m_{\text{Pl}}}\right)^2, \quad (12)$$

where $g = g_U \sqrt{2}$ is the relevant effective gauge coupling constant, with $g_U \simeq 0.5$ being the unified gauge coupling, and the function

$$B(x) = \begin{cases} 1.04 x^{0.195} & \text{for } 10^{-2} \lesssim x \lesssim 10^2 \\ 2.4/\ln(2/x) & \text{for } x \lesssim 0.01. \end{cases} \quad (13)$$

The mean inter-string separation at the time of formation is $p \xi(\phi_{\text{str}})$, where $p \simeq 2$ is a geometric factor [3,6]. This distance increases by a factor $\exp(N_{\text{str}})$ during inflation and by $(t_r/\tau)^{2/3}$ during inflaton oscillations, where $N_{\text{str}} = (1/m_{\text{Pl}}^2) \int_{\phi_e}^{\phi_{\text{str}}} V d\phi/V'$ is the number of e -foldings experienced by the strings, t_r is the reheat time, and τ is the time when inflation ends. The mean inter-string distance at cosmic time t after reheating is given by

$$d_{\text{str}} = p \xi(\phi_{\text{str}}) \exp(N_{\text{str}}) \left(\frac{t_r}{\tau} \right)^{\frac{2}{3}} \frac{T_r}{T}, \quad (14)$$

with T_r being the reheat temperature, the temperature T during radiation dominance given by

$$T^2 = \sqrt{\frac{45}{2\pi^2 g_*}} \frac{m_{\text{Pl}}}{t}, \quad (15)$$

and g_* accounting for the appropriate value of the effective number of massless degrees of freedom for the relevant temperature range. For the numerical example considered in Sec. 2, $T_r = 10^9$ GeV, $t_r \simeq 0.36$ GeV $^{-1} \simeq 2.37 \times 10^{-25}$ sec, and $\tau \simeq 1.26 \times 10^{-12}$ GeV $^{-1} \simeq 8.3 \times 10^{-37}$ sec. The string network re-enters the post-inflationary horizon at cosmic time t_F during radiation dominance if

$$d_{\text{str}}(t_F) = 2t_F. \quad (16)$$

After horizon re-entry, the strings inter-commute and form loops at any subsequent time t_i . These loops of initial length $l_i = \alpha t_i$ decay via emission of gravity waves, and the dominant contribution comes from the largest loops with $\alpha \simeq 0.1$ [18]. The gravitational waves can be decomposed into normal modes, and the redshifted frequency of a mode k , emitted at time \tilde{t} , as observed today, is given by [2]

$$f = \frac{a(\tilde{t})}{a(t_0)} \frac{2k}{\alpha t_i - \Gamma G\mu(\tilde{t} - t_i)}, \quad \text{with } k = 1, 2, 3, \dots \quad (17)$$

Here $\Gamma \sim 50$ is a numerical factor [8], $a(t)$ is the scale factor of the universe, and $t_0 \simeq 6.62 \times 10^{41}$ GeV $^{-1}$ is the present cosmic time. We express the stochastic gravity wave abundance with a present frequency f as

$$\Omega_{\text{GW}} = \frac{1}{\rho_c} \frac{d\rho_{\text{GW}}}{d\ln f}, \quad (18)$$

where $\rho_c = 3H_0^2 m_{\text{Pl}}^2$ is the critical density of the universe, H_0 denotes the present value of the Hubble parameter, and ρ_{GW} is the energy density of the gravity waves. The total gravity wave background coming from all modes is given by [2]

$$\Omega_{\text{GW}}(f) = \sum_k \Omega_{\text{GW}}^{(k)}(f), \quad (19)$$

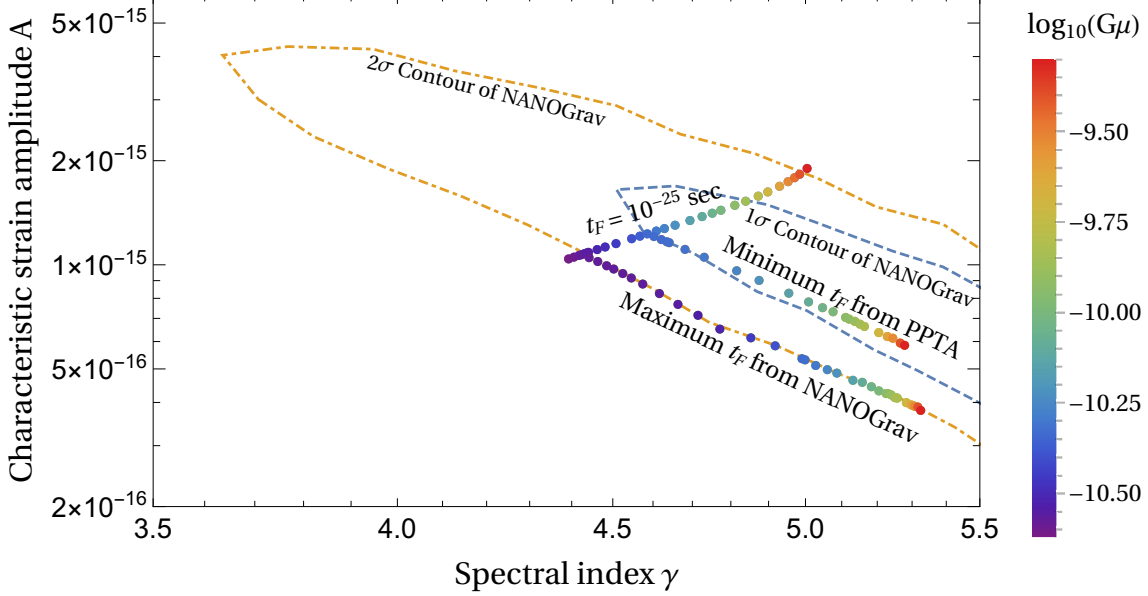


Figure 1: The amplitude A of the characteristic strain versus the spectral index γ for gravity waves from string loops of different $G\mu$ values is displayed on top of the 1σ and 2σ contours of NANOGrav [10]. The strings are assumed to: 1. be present in the horizon from a very early time (taken to be $t_F = 10^{-25}$ sec without loss of generality), 2. re-enter the horizon at the minimum time t_F required to satisfy the PPTA bound, and 3. re-enter the horizon at the maximum t_F allowed by the 2σ NANOGrav limit. The rainbow color code shows the variation of $G\mu$. The 1σ and 2σ ranges of $G\mu$ satisfying NANOGrav with very low t_F values are $[4.6, 14] \times 10^{-11}$ and $[2.7, 40] \times 10^{-11}$ respectively.

where

$$\Omega_{\text{GW}}^{(k)}(f) = \frac{1}{\rho_c} \frac{2k}{f} \frac{(0.1)\Gamma k^{-4/3} G\mu^2}{\zeta(4/3)\alpha(\alpha + \Gamma G\mu)} \int_{t_F}^{t_0} d\tilde{t} \frac{C_{\text{eff}}(t_i)}{t_i^4} \left(\frac{a(\tilde{t})}{a(t_0)} \right)^5 \left(\frac{a(t_i)}{a(\tilde{t})} \right)^3 \theta(t_i - t_F). \quad (20)$$

Here $\zeta(4/3) = \sum_{m=1}^{\infty} m^{-4/3} \simeq 3.60$, $C_{\text{eff}}(t_i)$ is found to be 0.5 and 5.7 for the radiation and matter dominated universe respectively [18], θ is the Heaviside step function, and the time t_i can be derived from Eq. (17).

We calculate the spectrum of gravity waves using Eqs. (19) and (20). Of course, \tilde{t} should be bigger than t_i since the loops cannot radiate before their formation at t_i . The ratios of the type $a(t)/a(t')$ ($t < t'$) are replaced by $(t/t')^{1/2}$ or $(t/t')^{2/3}$ if the period between t and t' lies entirely in the radiation or matter dominated period of the universe respectively. If $t < t_{\text{eq}} < t'$, where $t_{\text{eq}} \simeq 2.25 \times 10^{36} \text{ GeV}^{-1}$ is the equidensity time, i.e. the time at which the radiation and matter energy densities in the universe are equal, we split the time interval between t and t' and express these ratios as $(t/t_{\text{eq}})^{1/2}(t_{\text{eq}}/t')^{2/3}$. Needless to say, the integral in Eq. (20) takes into account all the loops that are created at $t_i > t_F$, and radiate a given mode characterized by k at $\tilde{t} < t_0$ contributing to the gravity waves with a given frequency f . The value of t_i is found from Eq. (17). Finally, the sum in Eq. (19) is taken over all the modes with $k = 1, 2, \dots, 10^5$.

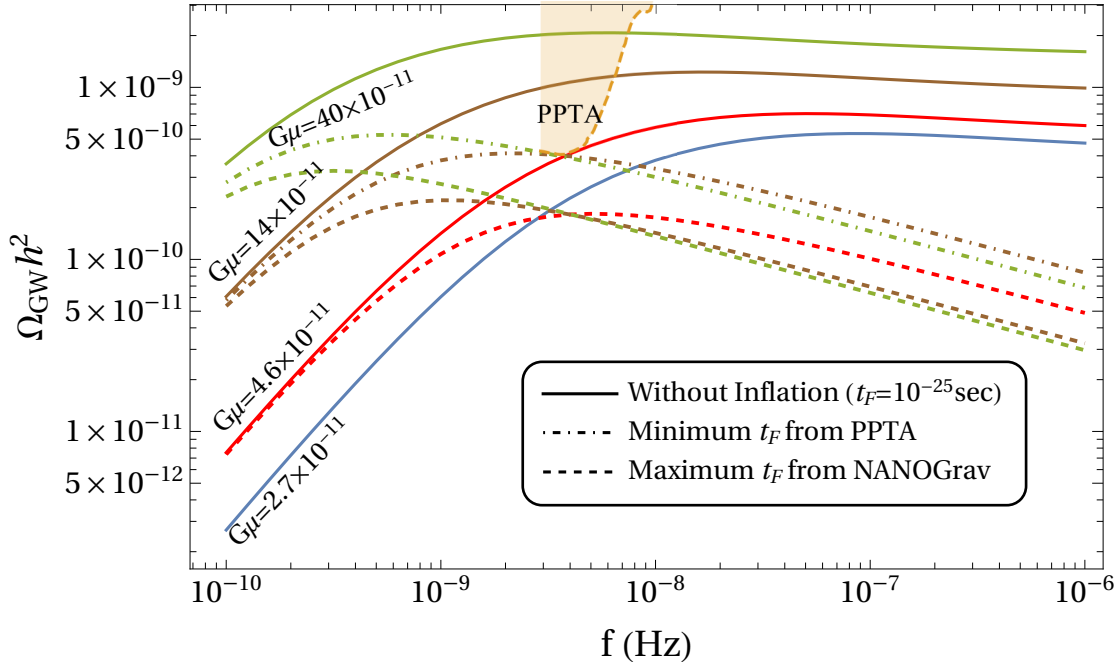


Figure 2: Gravity wave spectra with and without inflation for $G\mu = (2.7, 4.6, 14, 40) \times 10^{-11}$ (blue, red, brown, and green curves respectively). Without inflation (solid lines), the PPTA bound is violated for $G\mu > 4.6 \times 10^{-11}$. A minimum horizon re-entry time t_F of the strings is required so that the PPTA bound is satisfied for any given $G\mu$ in this range. The corresponding spectra are denoted by dash-dotted lines. On the other hand, there is a maximum t_F for the strings with $G\mu \geq 2.7 \times 10^{-11}$ allowing the 2σ NANOGrav limit to be met. The corresponding spectra are represented by dashed lines. The area excluded by PPTA is also shown.

4 Power-law Approximation for Gravity Waves and NANOGrav

In the NANOGrav experiment [10] the gravity wave spectra are expressed in a power-law form with characteristic strain

$$h_c(f) = A \left(\frac{f}{f_{\text{yr}}} \right)^\alpha, \quad (21)$$

where $f_{\text{yr}} = 1\text{yr}^{-1}$ is the reference frequency. This gives

$$\Omega_{\text{GW}}(f) = \frac{2\pi^2}{3H_0^2} f^2 h_c(f)^2 = \Omega_0 \left(\frac{f}{f_{\text{yr}}} \right)^{5-\gamma}, \quad (22)$$

where $\Omega_0 = (2\pi^2/3H_0^2)A^2 f_{\text{yr}}^2$ and $\gamma = 3 - 2\alpha$. We compute the gravity wave spectrum using Eqs. (19) and (20) within the frequency range $f \in [2.4, 12] \times 10^{-9}$ Hz, and fit the results to the power-law expression in Eq. (22) so as to calculate the amplitude A of characteristic strain and the spectral index γ . We then compare the calculated A and γ values with the NANOGrav 12.5 yr results [10]. In Fig. 1, we show the fitted values of A and γ for different values of $G\mu$ within the range $[2.4, 50] \times 10^{-11}$. We first take the time t_F at which the formation of the string

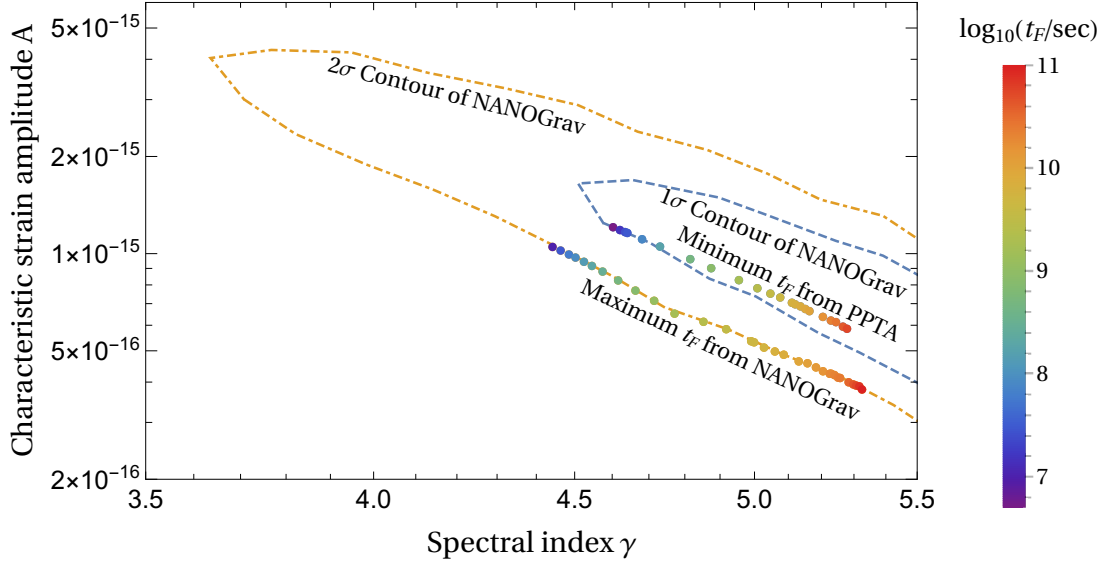


Figure 3: The amplitude A of characteristic strain versus the spectral index γ for gravity waves from string loops of different $G\mu$ values is plotted on the 1σ and 2σ contours of NANOGrav with the strings 1. re-entering the horizon at the minimum time t_F required from the PPTA bound, and 2. re-entering the horizon at the maximum t_F allowed by the 2σ NANOGrav range. The rainbow color code shows the variation of t_F .

loops starts to be very small, which would be the case without inflation. Although the results in this case are insensitive to the precise value of t_F , we set $t_F = 10^{-25}$ sec for definiteness. We find that the NANOGrav 12.5 yr data are well satisfied for $G\mu \in [4.6, 14] \times 10^{-11}$ and $G\mu \in [2.7, 40] \times 10^{-11}$ within the 1σ and 2σ limits respectively. The corresponding gravity wave spectra for $G\mu = (2.7, 4.6, 14, 40) \times 10^{-11}$ are shown in Fig. 2 by solid lines. We observe that without inflation, in which case t_F is very small, the PPTA bound [11] is in conflict with the NANOGrav results for $G\mu > 4.6 \times 10^{-11}$. In this case we consider higher values of t_F so that the spectrum satisfies the PPTA bound. In Fig. 2, the spectra corresponding to the minimum required value of t_F so that the PPTA bound is satisfied are represented by dash-dotted lines, and the spectra for the maximum t_F allowed by the 2σ limit from NANOGrav by dashed lines. The values of A and γ corresponding to the minimal t_F so that the PPTA bound is satisfied, and the maximal t_F allowed by the 2σ NANOGrav limit for $G\mu$ varying in the range $[2.7, 50] \times 10^{-11}$ are depicted in Figs. 1 and 3, with a rainbow color code for the variation of $G\mu$ and t_F respectively.

5 Inflation and Resolution of the Tension between PPTA and NANOGrav

We now return to the successful inflationary scenario summarized in Sec. 2. With different choices of the ratio α_{str}/g^2 between 0.1 and 14, we find the horizon re-entry time t_F of the

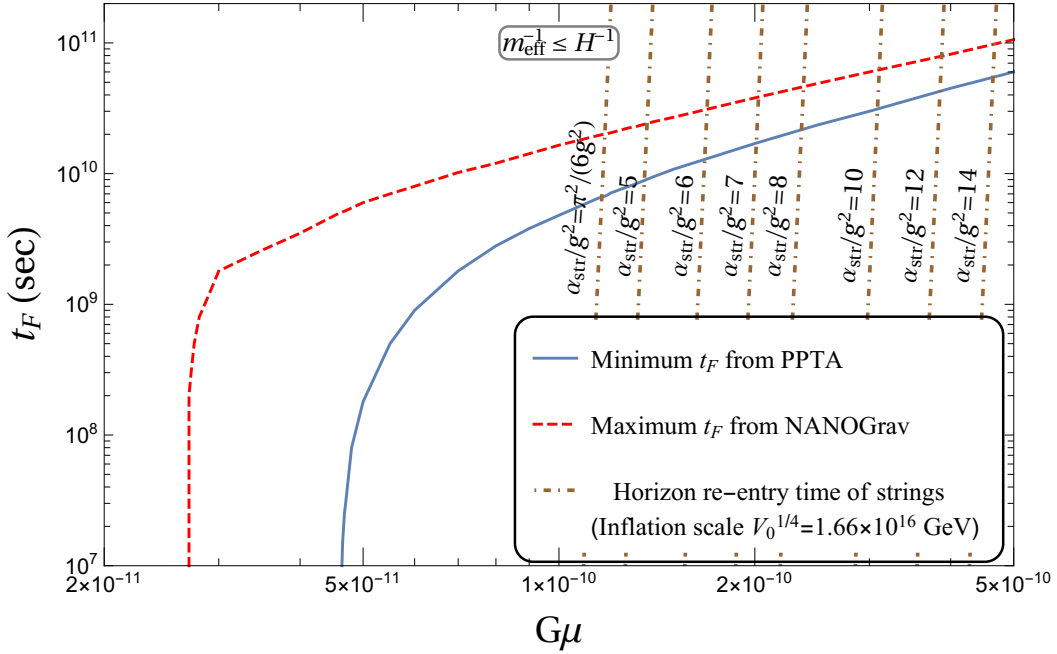
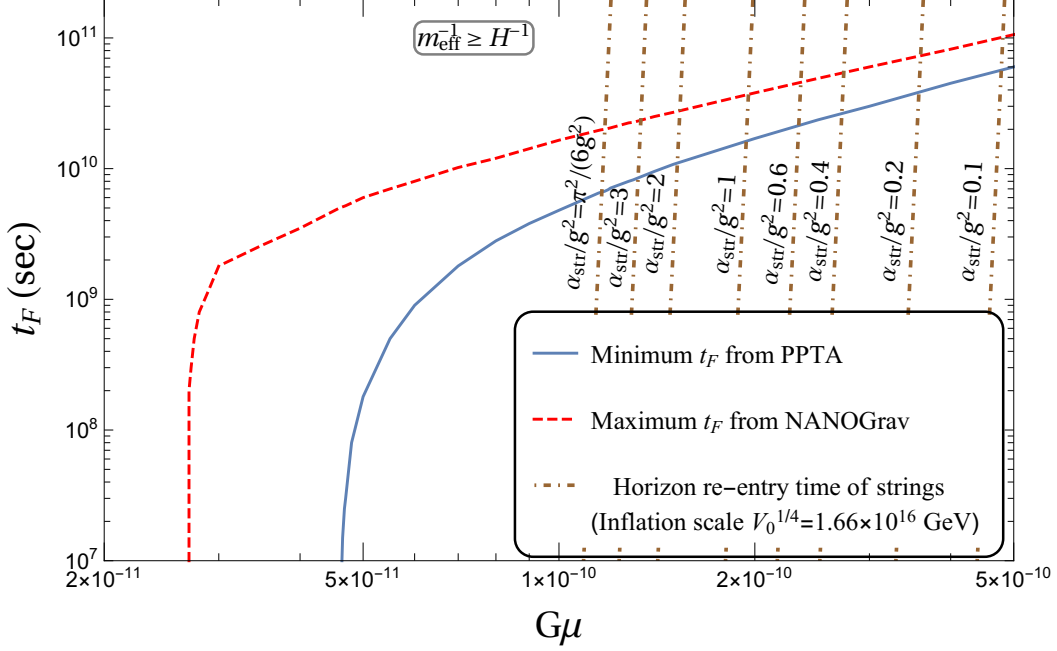


Figure 4: Horizon re-entry time of the strings as a function of $G\mu$ (brown dash-dotted curves) for different values of the ratio α_{str}/g^2 as indicated. In the upper (lower) panel $\alpha_{\text{str}} \leq \pi^2/6$ ($\alpha_{\text{str}} \geq \pi^2/6$) corresponding to $m_{\text{eff}}^{-1} \geq H^{-1}$ ($m_{\text{eff}}^{-1} \leq H^{-1}$). The solid blue lines depict the minimum t_F allowed by the PPTA bound. Notice that for $2.7 \times 10^{-11} \leq G\mu \leq 4.6 \times 10^{-11}$, t_F can be very small. The red dashed lines correspond to the maximum allowed t_F from the 2σ NANOGrav results. For $G\mu < 2.7 \times 10^{-11}$, the maximum t_F vanishes and so this region is excluded by NANOGrav.

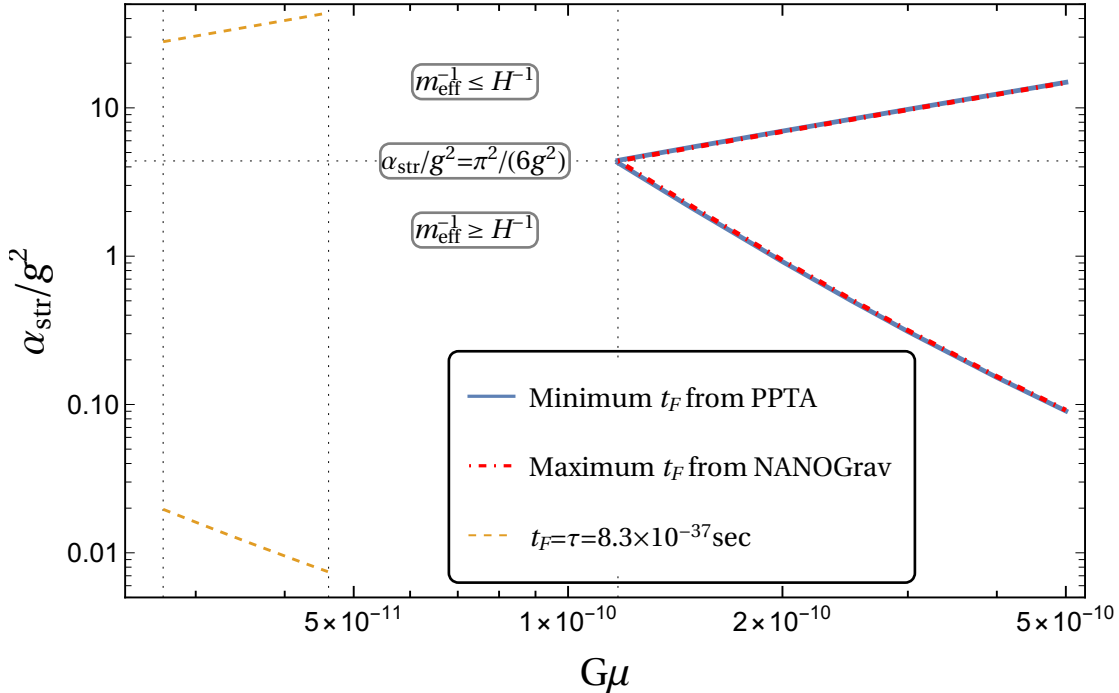


Figure 5: Allowed ranges of α_{str}/g^2 versus $G\mu$ for which the strings re-enter the horizon at times between the minimum t_F permitted by PPTA and the maximum t_F from the 2σ NANOGrav bound. For $2.7 \times 10^{-11} \leq G\mu \leq 4.6 \times 10^{-11}$, the lower and upper bounds on α_{str}/g^2 (brown dashed lines) correspond to $t_F = \tau$. $G\mu < 2.7 \times 10^{-11}$ is excluded by NANOGrav.

string network as a function of $G\mu$. The results are displayed in Fig. 4 superimposed on top of the minimum and maximum allowed values of t_F from PPTA and NANOGrav respectively. In the upper panel $\alpha_{\text{str}} \leq \pi^2/6$ and thus the correlation length $\xi = H^{-1}$. In the lower panel, on the other hand, $\alpha_{\text{str}} \geq \pi^2/6$ and thus $\xi = m_{\text{eff}}^{-1}$. The allowed values of α_{str}/g^2 and M_{str} for various $G\mu$ values are shown in Figs. 5 and 6 respectively. These values are compatible with the allowed ranges of t_F which satisfy both the PPTA and NANOGrav bounds. We observe that, in these figures, there exist two very narrow allowed strips corresponding to $\alpha_{\text{str}} \leq \pi^2/6$ and $\alpha_{\text{str}} \geq \pi^2/6$ for $G\mu \gtrsim 1.1 \times 10^{-10}$. For $2.7 \times 10^{-11} \leq G\mu \leq 4.6 \times 10^{-11}$ very small value of t_F are permitted. However, t_F cannot be made smaller than the time $\tau \simeq 8.3 \times 10^{-37}$ sec when inflation is terminated. This corresponds to a lower and an upper bound on α_{str}/g^2 in this range depicted in Fig. 5 by brown dashed lines. The corresponding upper and lower bound on M_{str} is depicted in Fig. 6 by brown dashed lines. For $2.7 \times 10^{-11} \leq G\mu \leq 4.6 \times 10^{-11}$, there is no conflict between PPTA and NANOGrav and thus inflation is not required. The range $G\mu < 2.7 \times 10^{-11}$ is forbidden by NANOGrav and no allowed solutions for α_{str}/g^2 and M_{str} are found in the range $4.6 \times 10^{-11} < G\mu < 1.1 \times 10^{-10}$. The number of e -foldings N_{str} experienced by the strings are also shown in Fig. 7. Note that N_{str} in the range $2.7 \times 10^{-11} \leq G\mu \leq 4.6 \times 10^{-11}$ can be arbitrary small. To summarize, we see that Coleman-Weinberg inflation can resolve the tension between the PPTA and recent NANOGrav measurements for $G\mu$ values in the range $1.1 \times 10^{-10} < G\mu <$

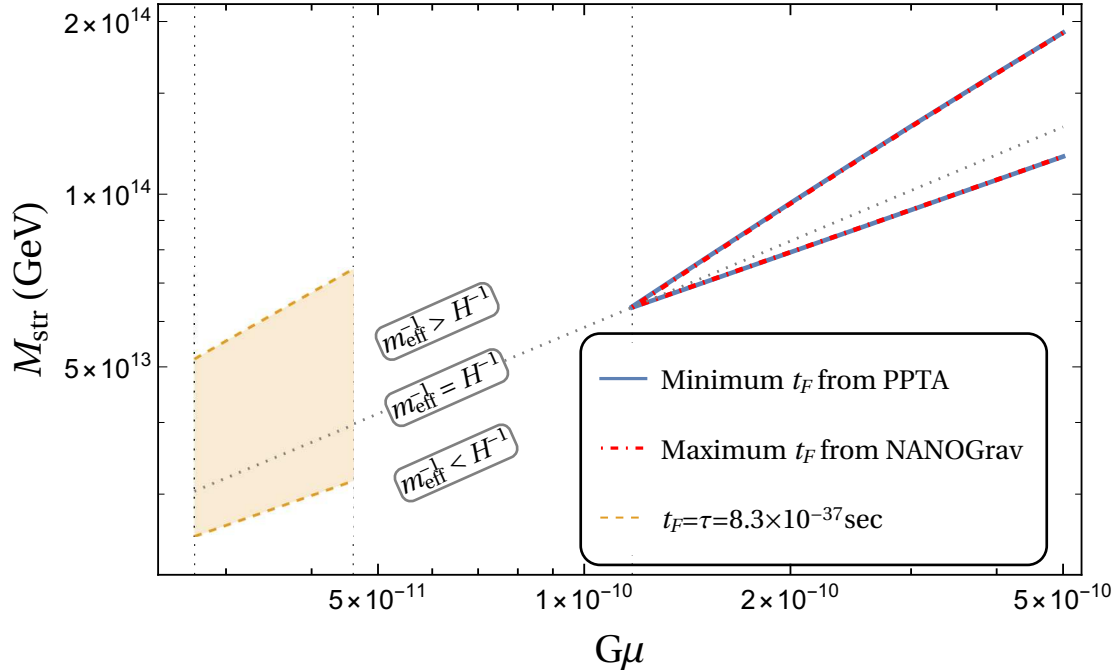


Figure 6: Allowed ranges of M_{str} for given $G\mu$ values so that the string network re-enters the horizon between the minimum t_F permitted by PPTA and the maximum t_F from NANOGrav. For $G\mu > 1.1 \times 10^{-10}$, there exist two narrow allowed strips corresponding to $m_{\text{eff}}^{-1} \geq H^{-1}$ ($\alpha_{\text{str}} \leq \pi^2/6$) and $m_{\text{eff}}^{-1} \leq H^{-1}$ ($\alpha_{\text{str}} \geq \pi^2/6$) as indicated. For $2.7 \times 10^{-11} \leq G\mu \leq 4.6 \times 10^{-11}$, the upper and lower bounds on M_{str} (brown dashed lines) correspond to $t_F = \tau$. In the region $4.6 \times 10^{-11} < G\mu < 1.1 \times 10^{-10}$, there exist no solutions for M_{str} , and $G\mu < 2.7 \times 10^{-11}$ is excluded by NANOGrav.

4×10^{-10} . The required values of M_{str} though lie in narrow strips. The PPTA and NANOGrav results are compatible in our inflation model in the range $2.7 \times 10^{-11} \leq G\mu \leq 4.6 \times 10^{-11}$ too, where inflation is though not needed to resolve the above tension.

As example, we consider the realistic non-supersymmetric $SO(10)$ model studied in detail in Ref. [6] which leads to the production of intermediate scale topologically stable cosmic strings. The GUT gauge symmetry in this model breaks via two intermediate steps corresponding to the scales M_I and M_{II} . Intermediate mass monopoles are associated with the first intermediate scale M_I and cosmic strings are produced during the second intermediate phase transition at the scale $M_{II} = M_{\text{str}}$. This model is linked to successful inflation with a Coleman-Weinberg potential for a gauge singlet real scalar inflaton. Moreover, it is compatible with gauge coupling constant unification, the constraints from proton decay, and other phenomenological and cosmological requirements. In Fig. 8, we depict the allowed region of the model in the plane of the two intermediate scales M_I, M_{II} for $V_0^{1/4} = 1.66 \times 10^{16}$ GeV derived from the corresponding region in Fig. 7 of Ref. [6] by restricting the value of $V_0^{1/4}$. This central value of $V_0^{1/4}$ corresponds to the unification scale $M_X = 3.89 \times 10^{16}$ GeV [6]. In Fig. 8, we also show the region which is compatible

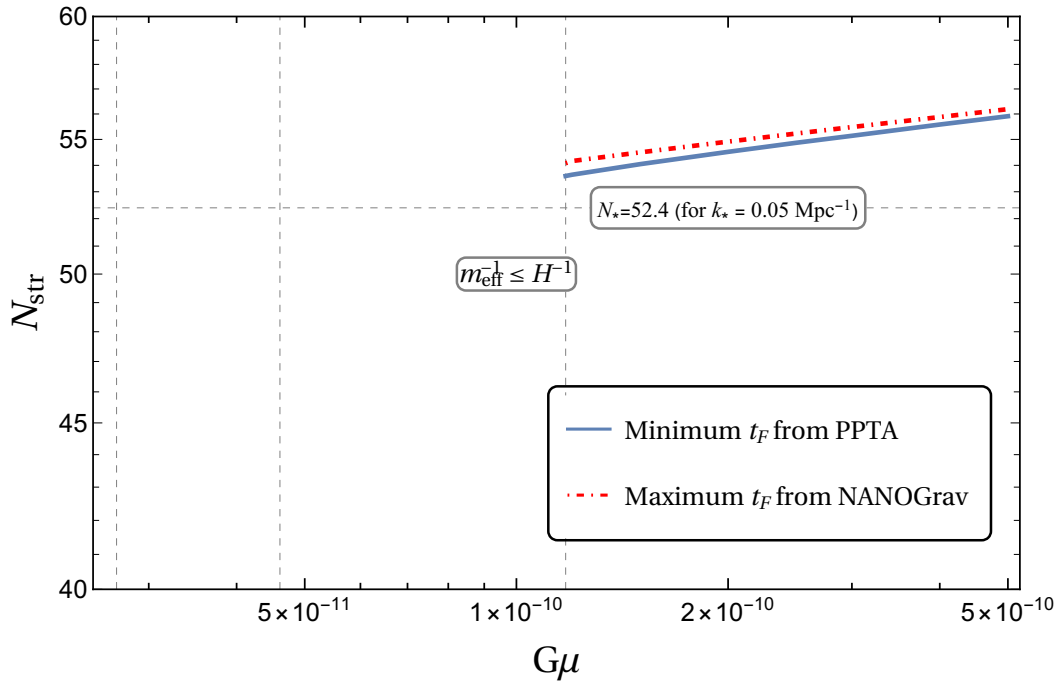
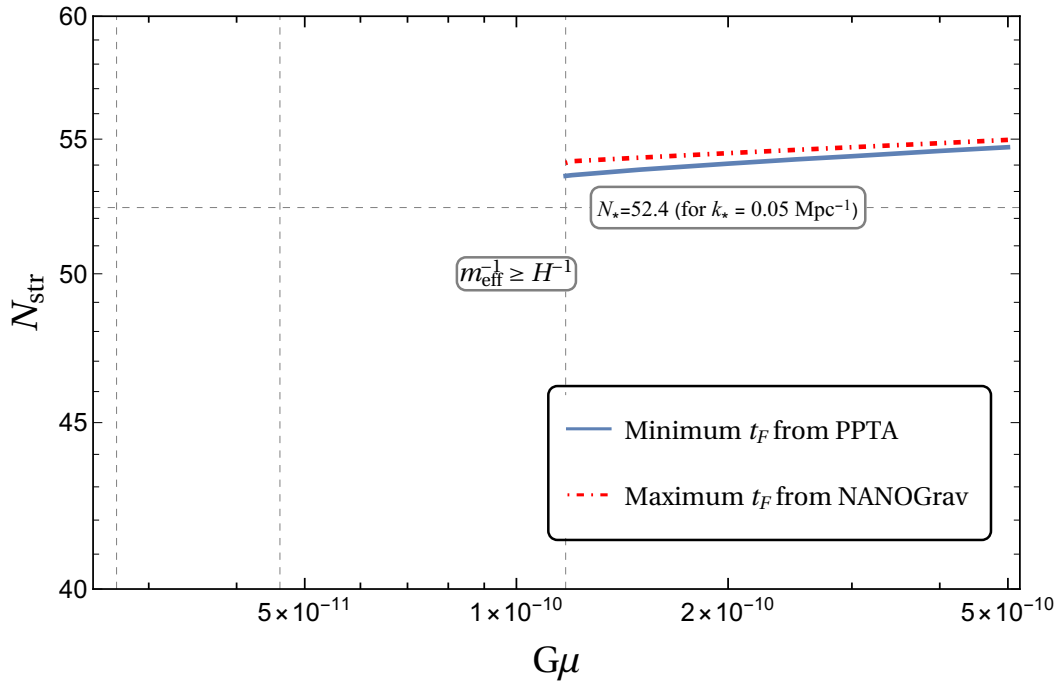


Figure 7: Allowed number of e -foldings N_{str} experienced by the strings for various $G\mu$ values so that the strings re-enter the horizon at times between the minimum and maximum t_F from PPTA and NANOGrav respectively. The upper (lower) panel corresponds to $\alpha_{\text{str}} \leq \pi^2/6$ ($\alpha_{\text{str}} \geq \pi^2/6$). In the range $2.7 \times 10^{-11} \leq G\mu \leq 4.6 \times 10^{-11}$, N_{str} can be arbitrary small.

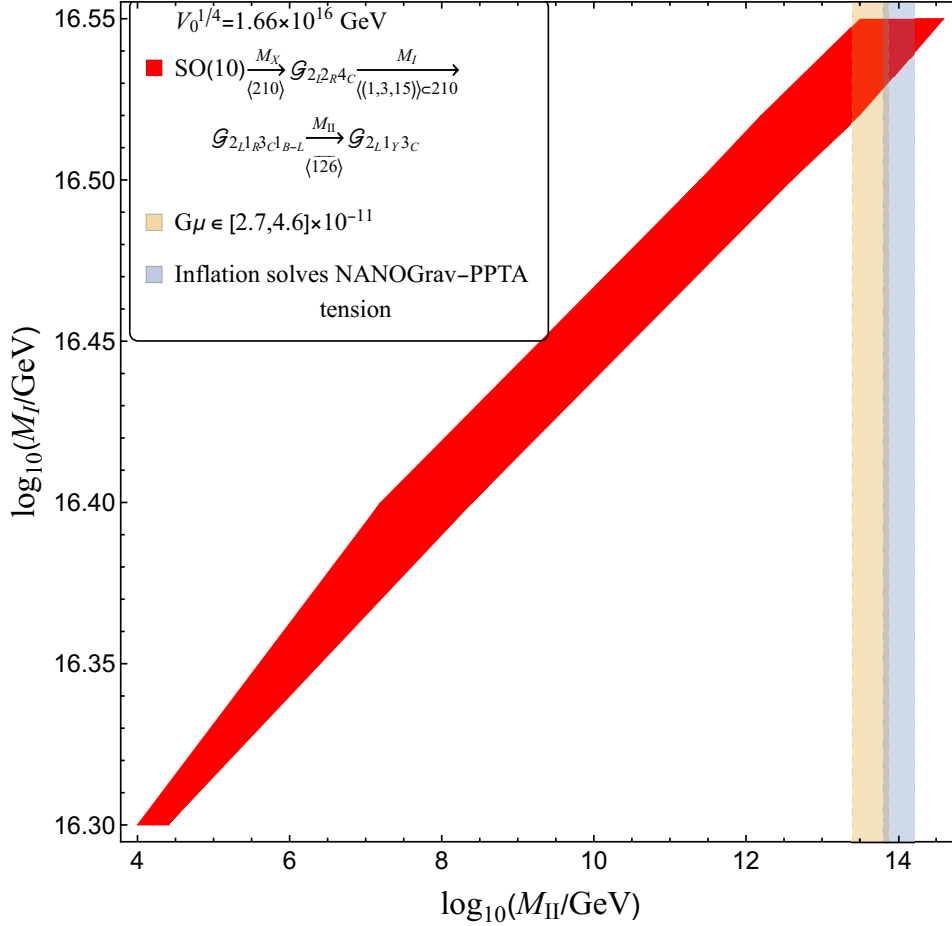


Figure 8: The allowed (red) area in the M_I , M_{II} plane for an $SO(10)$ model in Ref. [6] with successful Coleman-Weinberg inflation, topologically stable cosmic strings, and $V_0^{1/4} = 1.66 \times 10^{16}$ GeV (notation as in Ref. [6]). In the blue vertical strip, inflation resolves the tension between PPTA and NANOGrav for $1.1 \times 10^{-10} < G\mu < 4 \times 10^{-10}$. The brown vertical strip depicts the allowed M_{II} values for inflation and $2.7 \times 10^{-11} \leq G\mu \leq 4.6 \times 10^{-11}$. In this region though there is no tension between PPTA and NANOGrav and thus inflation is not required.

with both the PPTA and NANOGrav constraints (blue vertical strip) for $1.1 \times 10^{-10} < G\mu < 4 \times 10^{-10}$. Note that without inflation there is some tension between PPTA and NANOGrav in this region and thus inflation is important for its resolution. The brown vertical strip depicts the allowed values of M_{II} within the inflationary scenario for $2.7 \times 10^{-11} \leq G\mu \leq 4.6 \times 10^{-11}$. However, in this region there is no tension between the PPTA and NANOGrav results to start with and thus inflation is not required. We observe that the blue and brown regions overlap with the allowed (red) region of the model. Consequently, there exist ranges of model parameters where the tension between the PPTA and NANOGrav results is resolved. The allowed ranges of $G\mu$ for any given value of $M_{II} = M_{\text{str}}$ in the blue or brown strip can be easily derived from Fig. 6. Finally, we should note that the allowed model parameters which simultaneously satisfy the PPTA and NANOGrav constraints fulfill [6] the MACRO bound [19] on the flux of the magnetic

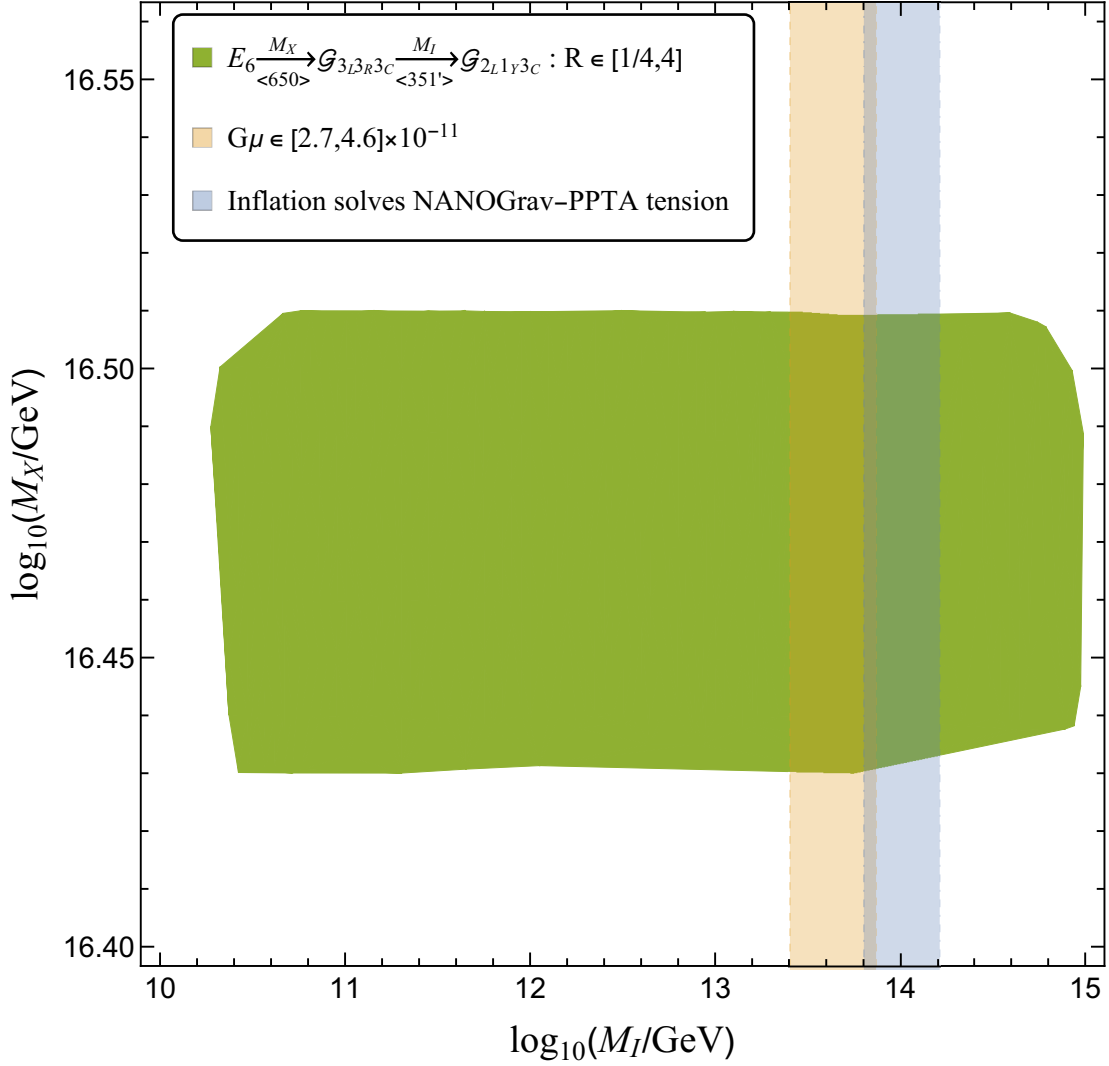


Figure 9: The allowed (green) region in the M_X, M_I plane for successful unification and inflation with a Coleman-Weinberg potential for the E_6 model with one-intermediate step of symmetry breaking (notation as in Ref. [6]). In the blue vertical strip inflation resolves the tension between PPTA and NANOGraV for $1.1 \times 10^{-10} < G\mu < 4 \times 10^{-10}$. The brown strip depicts the allowed M_I values in the inflation model for $2.7 \times 10^{-11} \leq G\mu \leq 4.6 \times 10^{-11}$. In this region though there is no tension between PPTA and NANOGraV and thus inflation is not required.

monopoles which were generated during the first intermediate phase transition. Actually, the resulting magnetic monopole flux turns out to be utterly low to be possibly measurable in the foreseeable future.

As another example with one intermediate step of symmetry breaking, we consider E_6 broken via the intermediate trinification symmetry $\mathcal{G}_{3_L 3_R 3_C} \equiv SU(3)_L \times SU(3)_R \times SU(3)_C$. The VEV of a scalar 650-plet along the D -parity [20] breaking and $\mathcal{G}_{3_L 3_R 3_C}$ -singlet direction breaks E_6 at a scale M_X . At this level, a scalar multiplet $(\bar{3}, 3, 1)$ from a 27-plet and another $(6, \bar{6}, 1) \subset 351'$ remain massless. The former contains the electroweak Higgs doublet, and the VEV of the lat-

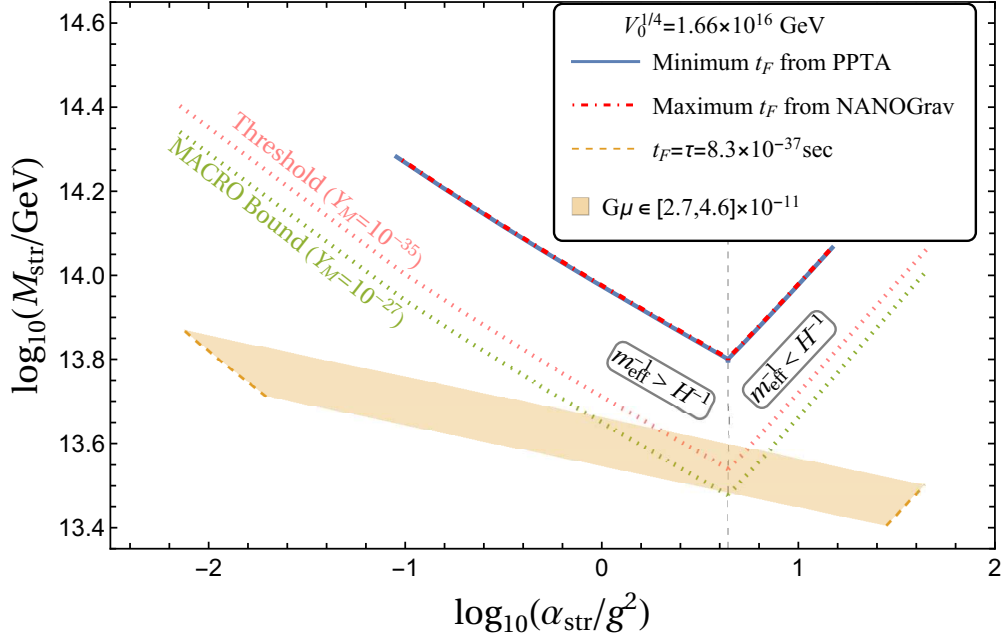


Figure 10: M_{str} versus α_{str}/g^2 for Coleman-Weinberg inflation with $V_0^{1/4} = 1.66 \times 10^{16}$ GeV. The solid blue line and the dash-dotted red line respectively correspond to the minimum t_F allowed by the PPTA bound and the maximum t_F compatible with the NANOGrav signal, for $1.1 \times 10^{-10} < G\mu < 4 \times 10^{-10}$. The brown region depicts the allowed M_{str} values in the inflation model for $2.7 \times 10^{-11} \leq G\mu \leq 4.6 \times 10^{-11}$. The dashed brown lines at the left and right boundaries of this region correspond to the strings that are created at the end of inflation. The green dotted line depicts the lower bound on M_{str} corresponding to the upper bound on the monopole flux from the MACRO experiment ($Y_M = 10^{-27}$), and the pink dotted line shows the adopted threshold for observability of the monopole flux ($Y_M = 10^{-35}$).

ter breaks the trinification symmetry to the standard model. This symmetry breaking produces topologically stable triply charged monopoles and cosmic strings at the same intermediate breaking scale M_I [3,21]. The β -coefficients at the two-loop level that govern the running of the three gauge couplings g_i ($i = 3L, 3R, 3C$) from M_I to M_X are given as

$$b_i = \begin{pmatrix} \frac{1}{2} \\ \frac{1}{2} \\ -5 \end{pmatrix}, \quad b_{ij} = \begin{pmatrix} 253 & 220 & 12 \\ 220 & 253 & 12 \\ 12 & 12 & 12 \end{pmatrix} \quad \text{with } i = 3L, 3R, 3C.$$

We have chosen the heavy gauge boson masses to be equal to the respective breaking scales, and the ratio R of the heavy scalar and fermion masses to the gauge boson masses to vary from 1/4 to 4. The solutions for successful unification and inflation with a Coleman-Weinberg potential are shown in Fig. 9 (green area). We have also shown the range of M_I (blue vertical strip) where the PPTA bound can be compatible with the NANOGrav signal for $1.1 \times 10^{-10} < G\mu < 4 \times 10^{-10}$, thanks to inflation which partially inflates the strings. The brown vertical strip depicts the allowed range of M_I within the inflation model for $2.7 \times 10^{-11} \leq G\mu \leq$

4.6×10^{-11} . However, we should keep in mind that inflation is not necessary for solving the PPTA-NANOGrav tension in this region. Although these strips were drawn for the central value of $M_X = 2.93 \times 10^{16}$ GeV corresponding to $V_0^{1/4} = 1.66 \times 10^{16}$ GeV, they are practically unaltered even if we allow M_X to vary within the range allowed by successful inflation. The blue and brown regions overlap with the allowed (green) region and, thus, there exist ranges of model parameters where the PPTA-NANOGrav tension is resolved.

We next examine whether the primordial monopole flux can be observable in this one intermediate step E_6 model. To this end, we construct Fig. 10 where we plot values of the string scale M_{str} allowed by gravity wave considerations versus α_{str}/g^2 . Assuming that monopoles are generated at the same scale, we also show the bounds on M_{str} from the monopole flux. The solid blue line and the dash-dotted red line respectively correspond to the minimum t_F allowed by the PPTA bound and the maximum t_F from the NANOGrav signal, for $1.1 \times 10^{-10} < G\mu < 4 \times 10^{-10}$. We observe that in this range of $G\mu$ there exist two very narrow allowed strips in our inflationary scenario. The brown region depicts the allowed M_{str} values within the inflation model for $2.7 \times 10^{-11} \leq G\mu \leq 4.6 \times 10^{-11}$. The dashed brown lines at the left and right boundaries correspond to the strings appearing at the end of inflation.

The green dotted line represents the upper bound on the magnetic monopole flux from the MACRO experiment [19] corresponding to a monopole abundance $Y_M = 10^{-27}$ [6, 22]. The pink dotted line, on the other hand, represents the adopted threshold for observability of the monopole flux ($Y_M = 10^{-35}$) [6]. The monopole abundance Y_M is calculated using Eq. (7.1) of Ref. [6] where m_{eff}^{-1} is replaced by the correlation length ξ . The two allowed strips in the range $1.1 \times 10^{-10} < G\mu < 4 \times 10^{-10}$ clearly satisfy the MACRO bound, but the predicted monopole flux is too low to be observable. Most of the brown region is excluded by the MACRO bound in our model as the monopoles do not undergo sufficiently large number of e -foldings. However, in the middle of this region around $\alpha_{\text{str}}/g^2 = \pi^2/6$ and between the green and pink dashed lines, the MACRO bound is satisfied and we have a potentially measurable monopole flux with the PPTA and NANOGrav results also simultaneously satisfied. In this region M_{str} is restricted in the range $13.48 < \log_{10}(M_{\text{str}}/\text{Gev}) < 13.67$. Consequently, the brown vertical strip in Fig. 9 is restricted to $\log_{10}(M_I/\text{Gev})$ values between 13.48 and 13.67. It is important to note that, although there is no PPTA-NANOGrav tension in this region to start with and thus inflation is not required for its resolution, it proves useful in adequately reducing the monopole flux and keeps intact the compatibility between the PPTA and NANOGrav results.

6 Conclusions

We discuss an apparent tension between the recent NANOGrav pulsar timing array data, which may support the presence of stochastic gravity waves emitted from cosmic strings with a dimensionless string tension $G\mu \simeq 2 \times 10^{-11} - 3 \times 10^{-10}$ at 95% c.l., and the previous pulsar timing array bound $G\mu \lesssim 4 \times 10^{-11}$ from the PPTA experiment. We propose a resolution of this tension by invoking primordial inflation which partially inflates the cosmic strings. The string

network re-enters the horizon at later times with a consequence that appropriately small string loops are not produced. This generally reduces the gravity wave spectrum with the reduction being much stronger at higher frequencies. The NANOGrav results can be made compatible with the earlier pulsar timing array bound provided that the strings re-enter the horizon at adequately late times. We present a concrete example of a realistic $SO(10)$ model supplemented by inflation with a Coleman-Weinberg potential. This model leads to the production of intermediate scale topologically stable cosmic strings that survive inflation, and we display a range of model parameters which enables us to resolve the tension between the NANOGrav and PPTA experiments. Finally, we present an E_6 model with one intermediate step of symmetry breaking in which there exists a range of parameters where both monopoles and strings survive inflation and there is no tension between the PPTA and NANOGrav results.

Acknowledgments

This work is supported by the Hellenic Foundation for Research and Innovation (H.F.R.I.) under the “First Call for H.F.R.I. Research Projects to support Faculty Members and Researchers and the procurement of high-cost research equipment grant” (Project Number: 2251). Q.S. is supported in part by the DOE Grant DE-SC-001380. R.M. is supported by the Senior Research Fellowship from University Grants Commission, Government of India. We thank Joydeep Chakraborty for his collaboration in the early stages of this work.

References

- [1] T.W.B. Kibble, G. Lazarides, and Q. Shafi, Phys. Lett. **113B**, 237 (1982).
- [2] Y. Cui, M. Lewicki, D.E. Morrissey, and J.D. Wells, Phys. Rev. D **97**, 123505 (2018); Y. Cui, M. Lewicki, D.E. Morrissey, and J.D. Wells, J. High Energy Phys. **01**, 081 (2019).
- [3] G. Lazarides and Q. Shafi, J. High Energy Phys. **10**, 193 (2019).
- [4] D. Matsunami, L. Pogosian, A. Saurabh, and T. Vachaspati, Phys. Rev. Lett. **122**, 201301 (2019); P. Auclair, D.A. Steer, and T. Vachaspati, Phys. Rev. D **101**, 083511 (2020); Y. Gouttenoire, G. Servant, and P. Simakachorn, J. Cosmol. Astropart. Phys. **07**, 032 (2020); Y. Cui, M. Lewicki, and D.E. Morrissey, Phys. Rev. Lett. **125**, 211302 (2020); S.F. King, S. Pascoli, J. Turner, and Y.-L. Zhou, Phys. Rev. Lett. **126**, 021802 (2021).
- [5] J. Ellis and M. Lewicki, Phys. Rev. Lett. **126**, 041304 (2021).
- [6] J. Chakraborty, G. Lazarides, R. Maji, and Q. Shafi, J. High Energy Phys. **02**, 114 (2021).
- [7] W. Buchmuller, V. Domcke, and K. Schmitz, Phys. Lett. B **811**, 135914 (2020); R. Samanta and S. Datta, e-Print:2009.13452 [hep-ph]; N.S. Pol et al. [NANOGrav Collaboration], e-

- Print:2010.11950 [astro-ph.HE]; S. Blasi, V. Brdar, and K. Schmitz, Phys. Rev. Lett. **126**, 041305 (2021).
- [8] A. Vilenkin and E.S. Shellard, Cosmic Strings and Other Topological Defects, Cambridge University Press (2000).
- [9] J.J. Blanco-Pillado, K.D. Olum, and X. Siemens, Phys. Lett. B **778**, 392 (2018).
- [10] Z. Arzoumanian et al. [NANOGrav Collaboration], Astrophys. J. Lett. **905**, L34 (2020).
- [11] R.M. Shannon, V. Ravi, L.T. Lentati, P.D. Lasky, G. Hobbs et al., Science **349**, 1522 (2015).
- [12] Q. Shafi and A. Vilenkin, Phys. Rev. Lett. **52**, 691 (1984).
- [13] G. Lazarides and Q. Shafi, Phys. Lett. B **148**, 35 (1984); Q. Shafi and V.N. Şenoğuz, Phys. Rev. D **73**, 127301 (2006).
- [14] V.N. Şenoğuz and Q. Shafi, Phys. Lett. B **752**, 169 (2016).
- [15] D.H. Lyth and A.R. Liddle, The primordial density perturbation: Cosmology, inflation and the origin of structure, Cambridge University Press (2009).
- [16] V.L. Ginzburg, Soviet Phys. Solid State **2**, 1824 (1961).
- [17] C.T. Hill, H.M. Hodges, and M.S. Turner, Phys. Rev. D **37**, 263 (1988); M. Hindmarsh, Prog. Theor. Phys. Suppl. **190**, 197 (2011).
- [18] J.J. Blanco-Pillado, K.D. Olum, and B. Shlaer, Phys. Rev. D **89**, 023512 (2014); J.J. Blanco-Pillado and K.D. Olum, Phys. Rev. D **96**, 104046 (2017).
- [19] M. Ambrosio et al. [MACRO Collaboration], Eur. Phys. J. C **25**, 511 (2002).
- [20] T.W.B. Kibble, G. Lazarides, and Q. Shafi, Phys. Rev. D **26**, 435 (1982).
- [21] J. Chakraborty, R. Maji, S.K. Patra, T. Srivastava, and S. Mohanty, Phys. Rev. D **97**, 095010 (2018); J. Chakraborty, R. Maji, and S.F. King, Phys. Rev. D **99**, 095008 (2019).
- [22] E.W. Kolb and M.S. Turner, The Early Universe, Front. Phys. **69**, 1 (1990).